Modeling of Birefringent Gires–Tournois Interferometer as a Double Ring Assisted Mach–Zehnder Electrooptic Modulator

Bráulio Fernando R Sakamoto (sakamoto@ita.br), William dos Santos Fegadolli (fegadolli@ita.br) and José Edimar Barbosa Oliveira (edimar@ele.ita.br)
Instituto Tecnológico de Aeronáutica – Divisão de Engenharia Eletrônica – Departamento de Microondas e Optoeletrônica. Praça Marechal Eduardo Gomes, 50 – Vila das Acácias – São José dos Campos city. São Paulo (SP) – Brazil. ZIP: 12228-900.

***Abstract* — Recently, optical modulators based on the Gires –Tournois interferometer (GTI), made of electrooptic materials, have attracted great interest because they may yield high linear dynamic range, hence play a significant role on the subject of signal processing in the field of microwave photonics, especially when applied in the field of electronic warfare receivers. This paper presents the modeling of a novel birefringent GTI modulator, which takes into account the front surface mirror reflectance, as a double ring assisted Mach–Zehnder modulator (RAMZI). Despites its rather reduced fabrication complexity, it is shown that a GTI modulator yields a dynamic range as high as that achieved with a mach more cumbersome RAMZI structure. Results of numerical simulations obtained with a Lithium Niobate ($LiNbO_3$) GTI which enables a push–pull operation with a single voltage source, are presented.**

***Index Terms* — Dynamic Range, Electrooptic Modulators, Gires–Tournois Interferometer, $LiNbO_3$, Microwave Photonics.**

I – Introduction

Optical modulators with high linear dynamic range play a significant role on the subject of microwave photonics signal processing. Aiming to meet this requirement, there have been numerous proposals made to improve the linearity of electrooptic modulators based on Mach–Zehnder interferometer (MZI), in the past few years [1], [2]. Modulators based on the so called Ring–Assisted Mach–Zehnder scheme (RAMZI), in which one or two ring resonators are coupled to the MZ arms, are strong candidates to fulfill this aim [3]. On the other hand, quite recently a rather simpler modulator schemes that combines the superlinear characteristics of Gires–Tournois interferometer with the sublinear characteristics of the Michelson interferometer to cancel the third order nonlinearity, was proposed [4].

This paper deals with the modeling of optical modulators based on birefringent Gires–Tournois interferometer (B-GTI), which consists of a Lithium Niobate ($LiNbO_3$) Pockels cell that enables a push–pull scheme operation with a single voltage source. It is shown that such B-GTI's transfer function emulates the RAMZI with a Spur–Free Dynamic Range (SFDR) as high as that of RAMZI modulator which comprises two identical rings coupled on each arm with a push–pull scheme operation. The properties of the B-GTI are investigated by the following parameters change: front surface mirror reflectance, interferometer length and Pockels cell half–wave voltage.

II – Mach–Zehnder Electrooptic Modulators

The schematic representation of an integrated optic Mach–Zehnder modulator, with $LiNbO_3$ substrate, is shown in Figure 1.

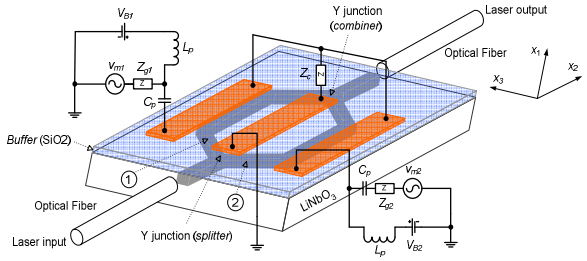

Fig. 1: Standard schematic representation of an integrated optic Mach–Zehnder modulator (MZM).

Regarding to the above shown schematic, it is well known that the incoming input laser beam, here after called input optical signal, feeds the input Y-junction of the MZ modulator, and then gives raise to the two optical beam which travels through the MZ's arms (which are labeled by ① and ②). As a consequence of the electrooptic effect, their propagation characteristics are independently controlled by the microwave modulating fields, whose spatial and temporal pattern depend on both, the microwave waveform and the electrodes geometry and relative positions with respect to the MZ arms. At the exit Y–junction the two optical signals are recombined and an intensity-modulated optical signal is obtained.

In order to obtain a first order approximation of the electrooptic modulator dynamic range, one can assume that the electrodes and the substrate are lossless and that the phase velocity matching requirement is achieved into the modulator microwave frequency range of operation. Furthermore, single mode operation is satisfied by both the fiber optic and the channel waveguide.

Bearing in mind the above given constraints, and considering push–pull driven operation, with a harmonic modulation waveform, one obtains following expression for the optical intensity at the MZ modulator illustrated in Fig. 1,

$$I_o^{(out)} = I_o^{(in)} \cos^2\left\{\frac{\pi}{V_\pi}\left[V_B + v_m \sin\left(\omega_m t + \phi_m\right)\right]\right\} \qquad (1)$$

where $I_o^{(in)}$ is the optical input intensity, V_B and V_π are, respectively, the DC bias voltage and the half-wave voltage of phase modulators that constitutes the MZM arms; ω_m and ϕ_m are, respectively, the frequency and phase of the modulator waveform.

Equation (1) reveals that the output intensity exhibits a non–linear dependence with respect to the amplitude of the modulation signal, as it is illustrated in Fig. 2.

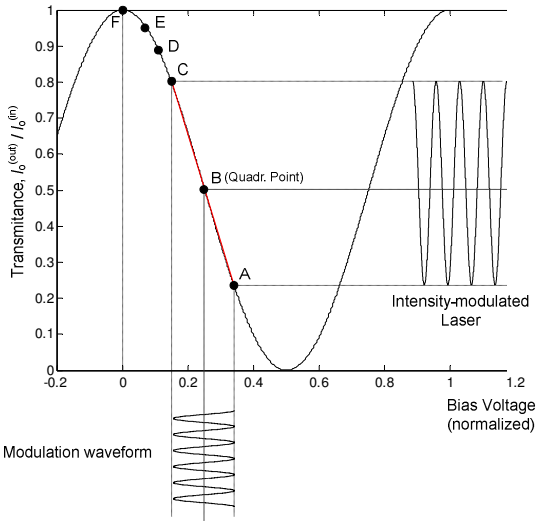

Fig. 2: Transfer function of a Mach–Zehnder modulator, push–pull driven by a harmonic waveform.

It is worthwhile to pint out that the non–linearity depends on the choice of the bier voltage, however, irrespective of such choice, the MZ modulator has a rather limited dynamic range, mostly due to the second order non–linear coefficient. Such feature plays a major role on the performance of MZ based analog signal processing devices.

Several approaches to linearization have been proposed, including cascaded MZ schemes, dual MZ schemes and directional coupler based modulators, among many others [2]. A rather interesting linearization scheme, based on a ring-assisted MZ, the so called Ring-Assisted Mach-Zehnder (RAMZ), as shown in Fig. 3, was proposed by Xie et al. [3].

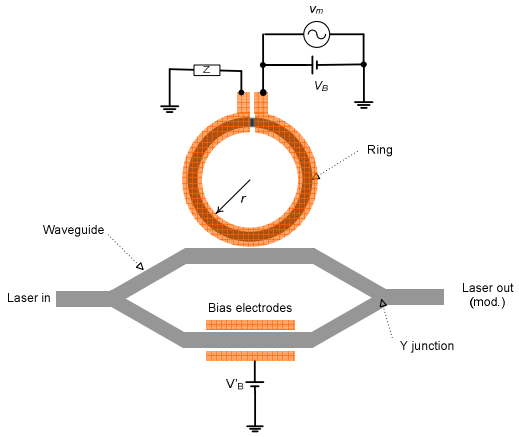

Fig. 3: Ring assisted Mach–Zehnder modulator (RAMZ).

The principle of operation of a RAMZ relies on the fact that the phase response of a ring resonator can be tuned by changing the coupling coefficient between the ring resonator and the optical waveguide, or Mach–Zehnder arm, to each it is connected. At a certain coupling strength, the transfer function a RAMZ becomes rather linear, namely its third-order derivative vanish at a given bias point of the transfer function. Such schematics do not require complicated electronics or optical control, once the appropriated coupling is determined by fabrication. To evaluate the linearity of a RAMZ, one can relay on the so called two-tone test to measures the magnitude of a third–order distortion product with respect to the first–order term [5]. As an example, using the parameters specified in [1], one concludes that a RAMZ provides a SFDR which is at least 18 dB higher than the one attained with a standard MZ modulator, as the one shown in Fig.1. On the other hand, regarding to the microwave bandwidth is the standard MZ configuration which displays better performance. However, one may be able to overcome such drawback by relaying on multi-ring assisted MZ schematics, in which both, the ring resonant frequencies and the coupling coefficients are properly chosen. Encouraging results on this regard have been obtained even with a Double-Ring Assisted Mach–Zehnder Modulator (D-RAMZ), as shown in Fig. 4 [3].

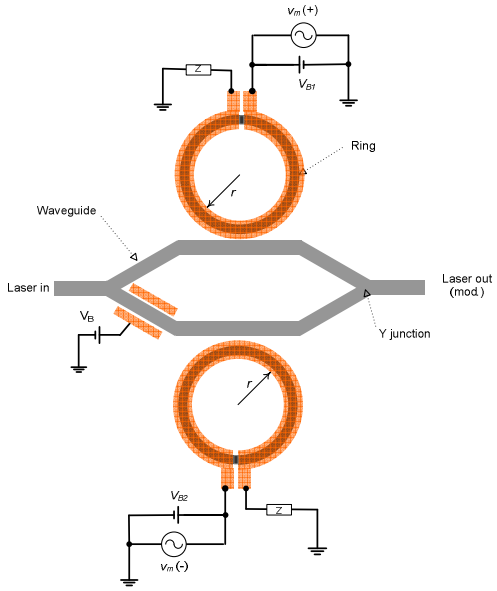

Fig. 4: Double-Ring assisted Mach–Zehnder modulator (D-RAMZ).

Like a conventional MZ, the D-RAMZ operates at a quadrature point, which means a quarter-period delay exists between the two arms. In addition, the effective optical length of the ring resonator is required to be an odd-multiple of the half operating wavelength in order to make it work in an off–resonance state.

It can be shown that if two identical rings are coupled on each arm of a MZ with a push–pull schemes operation, the output intensity of the D-RAMZ can be rewritten as a function of the refractive index change inside the ring resonators, and be quickly solved to obtain the optimized coupling coefficients. As far as SFDR is concerned, the D-

RAMZ's performance outplays both, the standard MZM and the single RAMZ (S-RAMZ) [3].

Quite recently, the results presented by many researches are pointing out towards the conclusion that a Gires–Tournois interferometer has the potential to enables rather simpler optical modulation schemes capable of yielding SFDR as good as the D-RAMZ. Motivated by such potential the authors of this paper undertook the challenge of developing a physics–mathematical model for a birefringent Gires–Tournois modulator aiming to be able, as far as SFDR is concerned, to identify its similarity with respect to the D-RAMZ based modulator.

III – Birefringent Gires–Tournois Modulator

The scheme of the proposed amplitude modulator, shown in Fig. 5, comprises rather standard optoelectronics components of electrooptic modulators (polarizer, circulator and waveplate) and a GTI made of a $LiNbO_3$ Pockels cell which has a front surface mirror reflectance Γ. In such modulator, the linearly polarized continuous–wave laser beam passes through an optical circular; the linearly polarized beam finally enters the z–axis of the $LiNbO_3$ crystal's principal axis perpendicularly at a polarization angle of 45° to the x–crystal's axis. Furthermore, the voltage source applied to the Pockels cell gives rise to an electric field parallel to the y–crystal's principal axis, which by its turn induces symmetrical changes to the refractive indexes associated to each optical normal polarization mode inside the $LiNbO_3$ crystal.

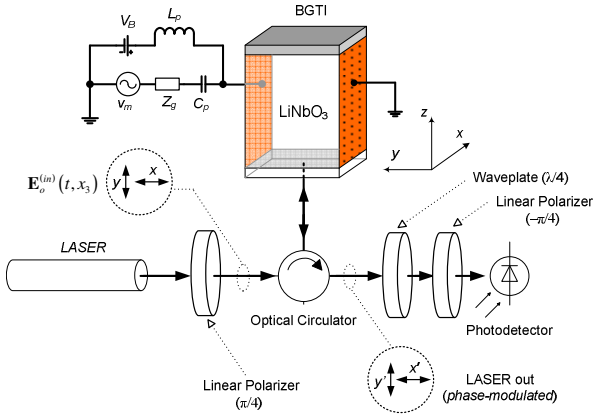

Fig. 5: Schematic representation of an electrooptic intensity modulator based on Birefringent Gires–Tournois interferometer.

Under the above stated conditions the refractive indexes seen by the x-polarized and y-polarized waves, respectively, inside the Pockels cell are:

$$\begin{cases} n_x = n_o + \dfrac{1}{2} n_o^{\,3} r_{22} E = n_o + \Delta n \\ n_y = n_o - \dfrac{1}{2} n_o^{\,3} r_{22} E = n_o - \Delta n \end{cases} \tag{2}$$

where n_o and r_{22} are, respectively, the ordinary refractive index and the relevant linear electrooptic coefficient of $LiNbO_3$ and E is the y–axis oriented modulation electric field.

Bearing in mind that the Pockels cell has a front surface mirror reflectance, Γ, one can readily shows that the x and y components of the total optical electric field steaming out of the B-GTI are determined by the following expression:

$$E_{x,y}^{(out)} = \frac{E_0 e^{j\omega t}}{\sqrt{2}} \left(\frac{\Gamma_{x,y} + e^{-j\phi_{x,y}}}{1 + \Gamma_{x,y} e^{-j\phi_{x,y}}} \right) \tag{3}$$

with:

$$\begin{cases} \phi_x = \dfrac{4\pi}{\lambda}(n_o + \Delta n) L = \phi_0 + \dfrac{4\pi \Delta n}{\lambda} L \\ \phi_y = \dfrac{4\pi}{\lambda}(n_o + \Delta n) L = \phi_0 - \dfrac{4\pi \Delta n}{\lambda} L \end{cases} \tag{4}$$

where E_0, λ and ω are, respectively the amplitude, the free space wavelength and the frequency of the CW laser electric field.

In order obtain some physical insight on the working principle of the B-GTI as an optical modulator as well as achieve some mathematical simplifications on its modeling, it is convenient to rewrite (3) in the following form:

$$E_{x,y}^{(out)} = \frac{E_0}{\sqrt{2}} \exp j\left[\omega t - \Phi_{x,y} \right] \tag{5}$$

where,

$$\Phi_{x,y} = -2 \operatorname{arctg}\left[\frac{1-\Gamma}{1+\Gamma} \tan\left(\frac{\phi_0}{2} + \frac{2\pi \Delta n}{\lambda} L \right) \right] \tag{6}$$

The above given results reveals one of the features which makes the B-GTI attractive as an optical modulator, namely, the fact that the phase of each optical electric field polarization of the out coming optical beam has a nonlinear dependence on both the front surface mirror reflectance, Γ, and the electrooptic induced refractive index change, Δn.

Furthermore, these phases displays behavior similar to those obtained by means of a double–ring assisted Mach–Zehnder interferometer, although they steam out of a device with demands a less complex fabrication technique [3].

Coming back to Fig. 1 and taking into account the static phase shift due to the optical wave plate, one obtains the following expression for the optical intensity at the output of the second optical polarizer:

$$\begin{aligned} I_{out} &= \frac{E_0^2}{2}\left[1 + \sin\left(\Phi_x - \Phi_y \right) \right] = \\ &= \frac{E_0^2}{2}\left[1 + \Phi_x - \Phi_y - \frac{1}{6}\left(\Phi_x - \Phi_y \right)^3 + \ldots \right] \end{aligned} \tag{7}$$

Equation (6) allows one to estimate the third-order

spurious-free dynamic range (SFDR) of a B-GTI based modulator by carrying out the well known two-tone third order intermodulation analysis. To this aim the modulation voltage is set as $v(t) = A(\operatorname{sen}\omega_1 t + \operatorname{sen}\omega_2 t)$. In order to be able to compare the results predicted in this paper with previously published one, as those presented in [3], one should make sure that $\phi_0 = (2k+1)\pi \quad (k = 0,1,2...)$. Under such condition, one expands Φ_x and Φ_y in powers of Δn. (only considering up to the third term here) to obtain:

$$\begin{cases} \Phi_x = \dfrac{4\pi}{\lambda}\dfrac{1-\Gamma}{1+\Gamma}\Delta n L + \dfrac{1}{3}\left(\dfrac{4\pi}{\lambda}\right)^3 \dfrac{(1-\Gamma)\Gamma}{(1+\Gamma)^3}(\Delta n L)^3 \\ \Phi_y = -\dfrac{4\pi}{\lambda}\dfrac{1-\Gamma}{1+\Gamma}\Delta n L - \dfrac{1}{3}\left(\dfrac{4\pi}{\lambda}\right)^3 \dfrac{(1-\Gamma)\Gamma}{(1+\Gamma)^3}(\Delta n L)^3 \end{cases} \quad (8)$$

As stated previously the above results shows a perfect agreement with the modeling of the two–ring assisted Mach–Zehnder interferometer, as discussed in [3]. Therefore, one should expect that a B-GTI based modulator offers a large improvement in modulation linearity with no requirements for complicated and precise fabrication process and electrical control.

IV – NUMERICAL SIMULATIONS

By combining equations (7) and (8), one readily obtains a rather useful expression for the output optical intensity of the modulator, as illustrated in Fig. 1, which explicit its dependence on both the front surface mirror reflectance, Γ, and the modulation voltage, $v(t)$, in the following form:

$$I_{out} = \frac{E_0^2}{2}\left\{1 - \operatorname{sin}\left\{4\operatorname{arctg}\left[\frac{1-\Gamma}{1+\Gamma}\cot\left(\frac{\phi_0}{2} + \frac{2\pi\Delta n}{\lambda}L\right)\right]\right\}\right\} \quad (9)$$

The graphic representation of this equation as a function of the static voltage level, the so called static characteristic curve, allows one to readily get a better view of the improvement in modulation linearity. For instance, as shown in Fig. 2, the optical intensity as a function of the voltage exhibits a significant higher linear behavior when $\Gamma = 0.5$ compared to the one attained when $\Gamma = 0$.

In order to further investigate the nonlinearity and third-order Spurious–Free Dynamic Range (SFDR) property of the B-GTI modulator, one has to expand its optical transfer function, as given by (9), in a Taylor series about a zero DC bias voltage. Such procedure was adopted in this paper, and a seven–order polynomial was considered a satisfactory approach. By substituting the two–tone voltage $v(t) = A(\operatorname{sen}\omega_1 t + \operatorname{sen}\omega_2 t)$ into the polynomial, the amplitude of the fundamental signal at angular frequency ω_1 and the intermodulation (IM) distortion at angular frequency $2\omega_1 - \omega_2$, which is usually named third–order intermodulation distortion, were calculated with multinomial theorem [6]:

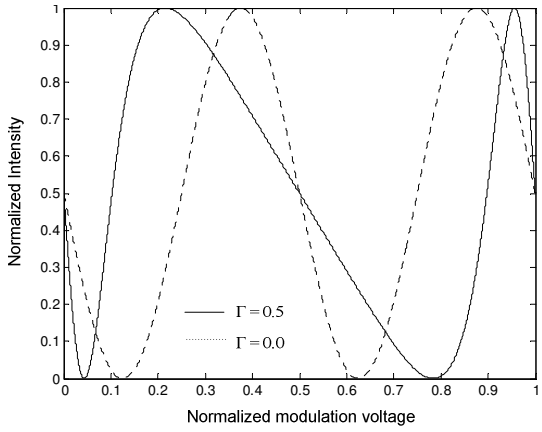

Fig. 6: Graphic representation of modulator static characteristic curve, as given by (9).

$$\begin{cases} I^{(\omega_1)} = a_1\dfrac{v_m}{V_\pi} + \dfrac{9}{4}a_3\left(\dfrac{v_m}{V_\pi}\right)^3 + \dfrac{25}{4}a_5\left(\dfrac{v_m}{V_\pi}\right)^5 + \dfrac{1225}{64}a_7\left(\dfrac{v_m}{V_\pi}\right)^7 \\ I^{(2\omega_1-\omega_2)} = \dfrac{3}{4}a_3\left(\dfrac{v_m}{V_\pi}\right)^3 + \dfrac{25}{8}a_5\left(\dfrac{v_m}{V_\pi}\right)^5 + \dfrac{735}{64}a_7\left(\dfrac{v_m}{V_\pi}\right)^7 \end{cases} \quad (10)$$

where the coefficients a_1, a_3, a_5 e a_7 only depend on the B-GTI front surface mirror reflectance, Γ.

Equations (9) and (10) describes that both the fundamental signal and the third–order intermodulation distortion at $2\omega_1 - \omega_2$ are influenced solely by odd-order nonlinearities and up to seventh–order nonlinearity of the B-GTI modulator can be taken into account to evaluate the dynamic range.

Owing to the rather cumbersome mathematical representation of the coefficients a_1, a_3, a_5 e a_7 of a B-GTI modulator, and recognizing that the largest third–order nonlinearity steams out of the a_3 coefficient, special attention is given to its dependence with respect to Γ, as it is illustrated in Fig. 7:

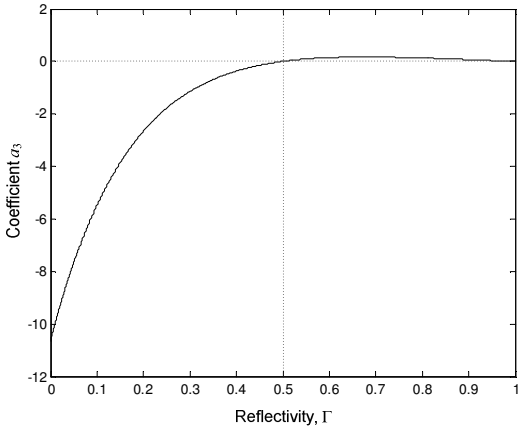

Fig. 7: Graphic representation of coefficient a_3 as a function of the B-GTI front surface mirror reflectance, Γ.

Figure 3 clearly confirms that the a_3 coefficient vanishes

at $\Gamma = 0.5$, which implies a high reduction of the third-order nonlinearity, hence the B-GTI exhibits significant improvement of the linearity, as has already been shown in Fig. 6.

To order to evaluate the linearity of a B-GTI, one has to calculate the intermodulation SFDR. The SFDR is defined as the ratio (usually expressed in dB units) of the fundamental signal power to IM power, when the IM power equals the noise level power. As an example, it is postulated a B-GTI scheme in which the noise floor is dominated by both the laser relative intensity noise and the shot noise to be –160 dBm. Fig. 4 shows the signal power and IM power of both a optimized B-GTI intensity modulator, with $\Gamma = 0.5$, and a conventional non-linearized one, which is equivalent to a B-GTI modulator with $\Gamma = 0.0$, as a function of the input signal power.

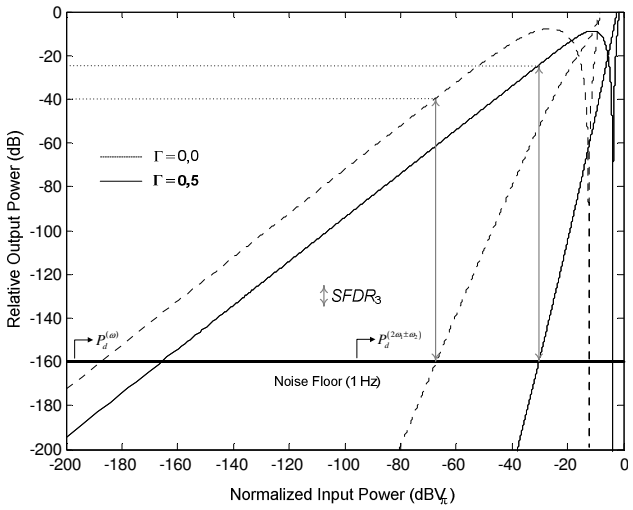

Fig. 4: Output signal power and IM power of both a B-GTI with $\Gamma = 0$ and an optimized B-GTI with $\Gamma = 0.5$, as function of the input signal power. The IM power of B-GTI varies as the fifth power of the input as does a RAMZI [3].

V – CONCLUSIONS

This paper dealt with the modeling of a novel birefringent GTI modulator (B-GTI), which takes into account the front surface mirror reflectance, as a Double-Ring Assisted Mach–Zehnder modulator (D-RAMZ). It is shown that a B-GTI modulator, despites its rather reduced fabrication complexity, yields a Spur-Free Dynamic Range (SFDR) as high as that achieved with a much more cumbersome RAMZI structure. For instance, it was shown that a B-GTI which relies on *z*-cut Lithium Niobate Pockels cell may enables a push-pull scheme operation with a single RF voltage source.

It is worthwhile to point out that among the many potential applications of B-GTI, steams out those related to optical sensors of electromagnetic field and optical signal waveform generators. Further studies on these regard are being undertaken by the authors.

ACKNOWLEDGEMENTS

The authors wish to acknowledge to Brazilian Air Force and Instituto Tecnológico de Aeronáutica (ITA) for the support and sponsorship given to the present research.

REFERENCES

[1] H. Tazawa, W. H. Steier, "Bandwidth of Linearized Ring Resonator Assisted Mach-Zehnder Modulator" *IEEE Photonics Tech. Letters,* vol. 17, no. 09, pp. 1851-1853, September 2005.

[2] B. B. Dingel, "Ultra Linear, Broadband Optical Modulator for High Performance Analog Fiber Link System" *IEEE International Topical Meeting on Microwave Photonics - MWP'04*, pp. 241-244, 4-6 October 2004.

[3] X. Xie, J. Khurgin, J. Kang, F. Chow, "Linearized Mach-Zehnder Intensity Modulator", *IEEE Photonics Tech. Letters,* vol. 15, no. 04, pp. 531-533, April 2003.

[4] N. Reingand, I. Shpantzer, T. Achian, A. Kaplan, A. Greenblatt, G. Harston, P.S. Cho, "Novel Design for the Broadband Linearized Optical Intensity Modulator", *MilCom 2003 IEEE*, vol. 2, pp. 1208 - 1212, October 2003.

[5] K. H. Brian and D. W. Dolfi, "Intermodulation Distortion and Compression in an Integrated Electrooptic Modulator", *Applied Optics*, vol. 26, No. 17, pp. 3676 – 3680, September 1987.

[6] Abramowitz M., and Stegun I.A. (Editors), "Handbook of Mathematical Functions", *Dover Publications*, NY, 1978.